American Journal of Nanotechnology & Nanomedicine

Research Article

Healing of Experimental Aseptic Skin Wound under the Influence of the Wound Dressing, Containing Silver Nanoparticles -

Alexander Yu. Vasil'kov[1], Ruslan I. Dovnar[2], Siarhei M. Smotryn[2], Nikolai N. Iaskevich[2] and Alexander V. Naumkin[1]*

[1]*Nesmeyanov Institute of Organoelement Compounds, Russian Academy of Sciences, 28 Vavilov st., 119991, Moscow, Russian Federation*

[2]*EI "Grodno State Medical University", 80 Gorky St., 230009, Grodno, Belarus*

***Address for Correspondence:** Alexander V. Naumkin, 28 Vavilov st., 119991, Moscow, Russian Federation, Russia, ORCID ID: orcid.org/0000-0001-5696-5723; E-mail: naumkin@ineos.ac.ru

Submitted: 05 December 2018 **Approved:** 26 December 2018 **Published:** 29 December 2018

Cite this article: Vasil'kov AY, Dovnar RI, Smotryn SM, Iaskevich NN. Naumkin AV. Healing of Experimental Aseptic Skin Wound under the Influence of the Wound Dressing, Containing Silver Nanoparticles. Am J Nanotechnol Nanomed. 2018; 1(2): 069-077.

ABSTRACT

A series of wound dressings, containing silver nanoparticles, based on medical gauze bandages, was obtained by the metal-vapor synthesis. Experimental laboratory rats were used to model aseptic skin wounds. The comparative dynamics of wound healing using a dressing containing silver nanoparticles and a conventional medical gauze dressing was studied. The influence of the silver-containing dressing material on the leukocyte number and blood leukogram, the main indicators of biochemical analysis of blood, was investigated. The wound dressings containing silver nanoparticles can accelerate the healing process of an experimental aseptic wound without significantly affecting the key indicators of the body homeostasis.

Keywords: Silver nanoparticles; Aseptic skin wound; Medical gauze dressing; Metal-vapor synthesis; XPS

INTRODUCTION

Nanoparticles are increasingly used in various fields of human activity, they are even called "material of the 21st century" [1]. Among all nanomaterials, metal nanoparticles and their oxides are widely used in medicine because of the wide spectrum of biological activity and unique physicochemical properties [2,3]. The Metal Vapor Synthesis (MVS) is an efficient means of purposeful synthesis of nanosized mono- and bimetallic particles and composites containing them. The modification of polymers with metal nanoparticles gives rise to several attractive functional properties, *e.g.*, magnetic, catalytic, antibacterial ones, etc. [4-7].

Silver, including in the form of nanoparticles, is used in medicine mainly due to its pronounced antibacterial, antifungal action [1,8], and a weak effect on eukaryotic cells [9]. The antimicrobial action of Silver Nanoparticles (Ag NPs) against Gram-positive (*S. aureus*) and Gram-negative bacteria species (*E. coli, Vibrio cholerae, Salmonella typhi,* and *P. aeruginosa*) has been proven [10]. However, it should be emphasized that the mechanism of the antimicrobial action of these nanoparticles is not fully understood. It is believed that Ag NPs can interact with the thiol groups of the peptidoglycan of the bacterial cell wall [11] or bind to the microbial DNA [12], causing its death. Eukaryotic cells in the cell wall do not have peptidoglycan, therefore, a much higher silver amount is necessary for their death [13].

One of the principles for the prevention of wound infection is the early use of broad-spectrum antimicrobials, primarily antibiotics [14]. However, antibiotic therapy has its negative features [15]. In this regard, the search for new methods for the prevention and treatment of wound infections, including the use of Ag NPs, is becoming promising. Drugs with antibacterial action can be placed on the dressing material and provide a local antimicrobial effect on bacteria [16]. It should be emphasized that despite the antibacterial properties of the dressing material containing Ag NPs, their effect on the course of the wound healing in the aseptic wound has not been investigated. Their possible effect on the number of leukocytes and the blood leukocyte formula has not been studied either.

To determine the correlation between the characteristics of materials containing Ag NPs and their bactericidal properties, the XPS is used. When analyzing materials containing metal nanoparticles by XPS it is necessary to take into account their increased chemical activity and relaxation effects during photoemission. The difference in conductivities and the secondary emission coefficients of the support and the nanoparticles can induce differential surface charging, which means that areas differing in these parameters can charge differently [17]. The reliability of the interpretation of the photoelectron spectra of non-conductive samples largely depends on the surface charge reference procedure, which is carried out in various ways.

Herein, we report our study, wherein the effect of medical gauze bandages containing Ag NPs, on the healing of aseptic skin wounds, the blood leukocyte count, leukocyte formula, and possible toxicity of Ag NPs to the liver, kidneys, and myocardium has been studied.

MATERIALS AND METHODS

The medical gauze dressing, produced in the Republic of Belarus (State Standard 1172-93) as a control and test samples were used. The test samples of gauze medical bandage were the dressing containing Ag NPs. MVS was used for the preparation of Ag containing bandage [18]. MVS is based on the interaction of extremely reactive atomic metals produced by evaporation under high vacuum conditions (10^{-4} – 10^{-5} Torr) with organics during their co-condensation on cooled walls of a reaction vessel. From the synthesis perspective, the resistive or electron beam evaporator is preferable. Scheme 1 shows a reactor for MVS.

Most typically, laboratory-scale researches are performed with small apparatus equipped with a glass reactor with a volume of 5-10 l and a resistive metal evaporator. Nowadays, MVS is an approved preparative technique capable of producing catalytically active systems, nanocomposite polymer materials or organometallic compounds that hardly can be synthesized via traditional routes.

The full preparation procedure can be formally divided into three steps. In the first step, the colloidal solution of nanoparticles in an organic solvent referred to as organosol (Ag-isopropanol) was prepared. The second step includes the impregnation of bandage with the organosol. In the third step, the solvent is removed and the Ag-containing bandage is dried in vacuo. TEM analysis of Ag-containing bandage showed that an average size of Ag NPs is 1.75 ± 0.25 nm [18].

XPS was employed to identify the chemical states of silver atoms and their amount. X-ray photoelectron spectra were collected with a Kratos XSAM-800 X-ray photoelectron spectrometer using an

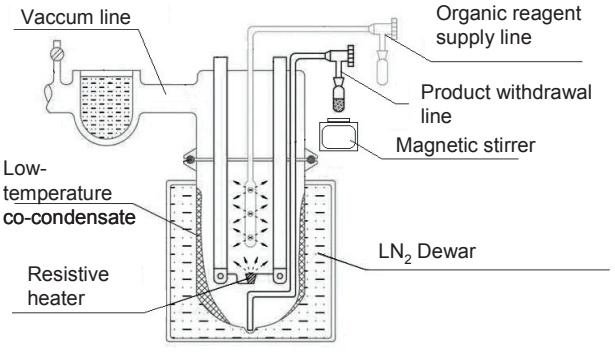

Scheme 1: The reactor for the metal vapor synthesis.

unmonochromated Mg Kα source (hν = 1253.6 eV). The anode power during measurements was within 90 W (15 kV, 6 mA), and the pressure in the sample analysis chamber was 10^{-8} Pa. The spectra were taken with the FRR mode at room temperature. Binding energies were referenced to the Au $4f_{7/2}$, Ag $3d_{5/2}$ and Cu $2p_{3/2}$ peaks, which were set at 84.0, 368.3 and 932.7 eV, respectively, with respect to the Fermi level. The secondary-electron-inelastic background was fitted with a straight line. A positive and negative bias voltage U_b was applied to the sample holder to discriminate electron emission from conductive and non-conductive areas. The analysis area was 9x17 mm^2. The samples were secured to a titanium holder in air using two-sided conductive adhesive tape and were in a good contact with the spectrometer. No pretreatment was applied before recording spectra.

As it was mentioned above, when interpreting the photoelectron spectra of nanoparticles, some factors such as the surface charging, the dependence of the photoelectron peak width on the chemical state and size of metal nanoparticles, differential charging and the use of reliable reference data and procedures that allow discriminate Ag^+ and Ag^0 states should be taken into account. Since the properties of the Ag NPs/bandage nanocomposite used for medical applications largely depend on the electronic state of the metal phase, this work presents an approach to the analysis of Ag black photoelectron spectra, which differs from that considered elsewhere [18].

In the study of the chemical state of silver atoms in various compounds and composites one of the important problems is discrimination between Ag^0 and Ag^+ states. The solution to this problem for massive samples can be found in [19-24] and references therein.

There is a large number of papers for X-ray analysis of Ag/cotton, Ag/cellulose and Ag/bandage systems used for medical applications. Table 1 shows a compilation of the characteristics of photoelectron spectra [25-35].

As can be seen from the presented data, when charge reference is according to the C 1s spectrum of adventitious carbon the range of 284.6-285.0 eV is rather large enough to discriminate between Ag^0 and Ag^+ states in the Ag 3d spectra. It appears that a more accurate accounting of surface charging can be carried out on the basis of the binding energy of the C-OH cellulose group, which is assigned a binding energy of 286.73 eV [36]. So, when adjusting the surface charge for the C-OH group [34] and making the amendment according to [36] the binding energy of the Ag $3d_{5/2}$ peak should be 368.33 eV. Earlier [37], it was noted that binding energies of 368.327 or 368.299 eV are most reliable data for Ag $3d_{5/2}$ peak when Al Kα or Mg Kα excitations are used. Therefore, the binding energy of 368.33 should be assigned to Ag^0 state. However, using the corresponding Auger parameter of 724.3 eV and compare it with value of 726.1 eV related to Ag^0 state He et al made wrong conclusion. It means that evaluations based on binding energy and Auger parameter are in contradiction. Other words, in case of inhomogeneous sample the Ag 3d photoelectrons and Ag MNN Auger electrons leave the sample from different information depths. The Ag MNN Auger electrons are more surface sensitive than Ag 3d photoelectrons. They evidence that at near surface the silver atoms are presumably in Ag^+ state or Ag NPs have core-shell structure $Ag^+@Ag^0$.

A number of papers present an incorrect statement that the oxidation of silver leads to a positive chemical shift [30-32]. When the spectrum was fitted with some Gaussian components [27], the fact that the Ag $3d_{5/2}$ peak of the Ag^0 state can be almost two times smaller than that of the Ag^+, 0.63 and 1.1 eV, respectively [23] state was not taken into account. However, despite the above features of the interpretation of photoelectron spectra, the use of controlled differential charging makes it possible in some cases to discriminate the Ag^+ and Ag^0 states with a high degree of reliability. It was previously used for this system [18]. Below are the data obtained using this technique, which allowed us to obtain information on the chemical state of silver atoms by analysis of the C 1s and O 1s spectra.

For the study, 54 outbred adult white rats (males) with an average weight of 224.5 g at the age from 6 months to 1 year, obtained from the vivarium of the EI "Grodno State Medical University" were used. 48 animals were operated. All of them were used to model of a full-layer plane aseptic skin wound. Before the experiment, the animals

Table 1: Binding energies of photoelectron peaks and kinetic energies of Auger peaks of Ag containing composites.

	Ag $3d_{5/2}$	Ag $3d_{3/2}$	$M_4N_{45}N_{45}$	Ag $3d_{5/2}$ + $M_4N_{45}N_{45}$	Cal	State		Ref
Ag/cotton	368.02	374.24			284.8	Ag^0		25
TiO_2@Ag/silk	368.0	374			284.6	Ag^0		26
TiO_2@Ag	367.0	373			284.6	Ag^0		27
Ag/cotton	368.7 368.1 367.8				284.8	Ag^0 Ag^+ Ag^{2+}	Identical FWHM	28
Ag/cotton	368.2 367.0	373.4 374.3			284.6	Ag^0 Ag^+	~FWHM	29
Ag/cotton	368	374			284.8	Ag^0		30
Ag/cotton	368.4	374.2			284.6	Ag^+ Ag^{2+}		31
Ag/cotton	370.1	376.2			285.0	Ag^+ Ag^{2+}		32
Ag/wool	368.3 - 368.7 369.3 - 370.1				285.0	Ag^0 Ag^+		33
Ag/cellulose	368.1		356.2	724.3	286.5	Ag^0		34
Ag/cellulose	368.3 367.6 367.9	374.3 373.6 373.9			284.8	Ag^0 Ag^+ Ag^+		35

were carefully examined for the presence of visible pathology and signs of disease. The animals with the identified pathology were culled and were not included in the experiment. 48 rats were divided into 2 groups: 24 rats were tied with an ordinary dressing whereas for other 24 rats, a dressing with Ag NPs was used. In each group, 6 animals were taken out on the 3rd, 7th, 14th, and 21st day of the experiment. The group of 6 intact animals was used to determine biochemical parameters and leukocyte blood.

All stages of the experiment were performed under conditions of adequate anesthesia with the permission of the Ethics Committee of the EI "Grodno State Medical University" and in accordance with the "European Convention on the Protection of Vertebrate Animals used for experiments or for other scientific purposes" (Strasbourg, 1986). Operations and animal ligation were performed under aseptic conditions in the Operating room of the Department of operative surgery and topographic anatomy of the Grodno State Medical University.

A model of a full-ply aseptic plane wound was created for all operated animals in the back area. Initially, under intramuscular ketamine anesthesia (0.5 ml of a 5 % solution), wool was shaved along the vertebral line on the back of animals in the interscapular region. After double processing the area of manipulation with the antiseptics, a previously sterilized safety chamber with a lid was stitched in order to create tightness, prevent possible injury to the wound and contamination by surrounding microorganisms, and to fix the dressing material. The safety chamber was a cylindrical base having openings for suture threads, a lid and a clamp. At the lower edge of the cylinder base opposite each other there were flat cuttings similar to the rat back and holes for suture threads. The cap on the inner surface had a stop device to prevent the dressing from moving. The lid was attached to the base with a clamp.

Then, iodine was applied to a sterile plastic piston, the diameter of which was 0.5 cm smaller than the internal diameter of the safety chamber, and the contour of the future wound was imprinted with a piston. In the indicated boundaries, the skin, subcutaneous tissue and superficial fascia were dissected with a scalpel. The wound surface formed in this way was smaller than the internal diameter of the safety chamber and was in the created insulating ring from the external environment until the end of the experiment with the animals.

The rats were kept at a natural change of day and night. The animals were synchronized by feeding under standard vivarium conditions in individual cells. This excluded their injury from other individuals, including the gnawing of fixing threads.

Immediately, after creating the aseptic wound model, a sterile medical bandage was placed in the safety chamber hemmed in the area of its location; the sterile medical bandage covering the entire wound surface with a 0.5 cm overhang of the wound edges: a gauze medical dressing in the control group, a gauze medical dressing with Ag NPs in the test one. Sterilization of the test and control samples was carried out by the method of autoclaving at 121°C for 16 minutes with the vacuum autoclave Cliniklav-25. Bandaging of animals was performed daily under ketamine anesthesia, during which the medical dressing was removed, the wound was photographed and the dressing was replaced with a new sterile one.

To determine the wound lesion area, the latter was photographed with a digital camera, the image was transferred to a computer, calibrated, and the area was evaluated using Scion Image 4.0 (NIH, USA). The results were expressed as a percentage of the initial area. The day of the injury was considered the zero day of the experiment.

In order to determine the effectiveness of wound treatment, on the 3rd, 7th, 14th, 21st day from the beginning of the experiment, the material was collected for the study with simultaneous breeding of rats from the experiment (6 individuals) from each group. Removal of animals from the experiment was carried out by decapitate. On the 14th day, tissues from wounds, blood, samples of the liver, kidneys and heart were taken. For the biochemical analysis, 0.5 ml of blood serum was taken, after which the Konelab 30i automated biochemical analyzer was used to determine the main biochemical parameters, such as ALT (IFCC method 37°), AST (IFCC method 37°), urea (urease method), creatinine (Jaffe method), total protein (biuret method), bilirubin (Indrashek modified method), and glucose (glucose oxidase method).

The count of blood leukocytes and the quantitative assessment of the main cell types (leukogram) were carried out using microscopic examination. The number of blood leukocytes was determined using the Goryaev counting chamber according to the standard technique. The leukocyte formula was counted in blood smears stained according to Romanovsky. Additionally, the leukocyte shift index was determined according to Yabuchinsky and the leucointoxic index using the following formulas [38].

$$\text{Leukocyte shift index by Yabuchinsk y} = \frac{E + B + S + Se}{L + M} \quad (1)$$

$$\text{Leucointoxic index} = \frac{My + Y + P + S + Se}{E + B + L + M} \quad (2)$$

Where, E is the number of eosinophils, B is the number of basophils, S is the number of stab neutrophils, Se is the number of segmented neutrophils, L is the number of lymphocytes, M is the number of monocytes, My is the number of myelocytes, Yu is the number of young neutrophils, and Pl is the number of plasma cells.

The areas of wound, liver, kidney and heart tissue (1/4 Inch × 1/4 Inch) of the rats were fixated in 10% buffered formalin (0.17 us fl oz), dehydrated in ascending alcohols, embedded in paraffin and stained with hematoxylin and eosin or picrofuxin according to Van Gieson. After that, a microscopic examination was performed under a light microscope.

Statistical processing of the results was carried out using Statistica 11.0 code. Differences between groups were assessed using the non-parametric Mann-Whitney U-test at a given 5% level of significance.

RESULTS

To discriminate between Ag^0 and Ag^+ states by XPS we have used the mode of controlled differential charging. As a rule, differential charging is considered as negative effect. To avoid it a flood gun emitted low energy electrons to the sample studied is used. However, differential charging can be used as a positive tool because it can help to discriminate electron emission from conductive and non-conductive areas. It is well known that silver oxides are semiconductors, while silver is a conductor. Therefore, using controlled differential charging it may be possible to discriminate between Ag^0 and Ag^+ states.

A positive and negative bias voltage $U_b = \pm 7V$ was applied to the sample holder to discriminate electron emission from conductive and non-conductive areas. When a positive voltage is applied, the

fluxes of electrons emitted from the foil window of the x-ray gun and stray electrons increase and compensate the surface charging. The photoelectron peaks related to conductive areas will shift by U_b value, while the shift of those related to non-conductive areas will be less than U_b value. The latter mainly depends on such parameters as secondary emission coefficient and electrical conductivity. When a negative voltage is applied the flux of the electrons compensating the surface charge decreases, while the energy interval between photoelectron peaks related to conducting and non-conductive areas increases.

Figure 1 shows the O 1s and C 1s spectra of Ag black measured at different U_b without (a) and with correction by U_b (b). The spectra are normalized by area under the spectral line. Such normalization means that the spectra related to the same number of carbon atoms. It is clearly seen that relative intensity of C-C/C-H state is less at U_b = 0 and -7 V than at U_b = +7 V. This is due to a decrease in the flow of stray electrons and an increase in charge in areas with low conductivity. The surface charging leads to a shift of part of the signal to the high energy region, which corresponds to the signal from the CO_x groups. Since the spectra are traditionally recorded at U_b = 0, in such cases the signal corresponding to the C-C/C-H state can be assigned to C-O bonds. A similar phenomenon is observed in the O 1s spectra, in which the relative intensity and binding energy of the Ag-O state weakly depend on U_b. This result additionally indicates a low concentration of oxidized silver and that the oxygen is located on silver particles. Otherwise, a shift of the signal to the region of high binding energies would be observed.

The binding energy of the C-C/C-H state deconvoluted in the C 1s spectra depends on U_b in a specific way, at U_b = 0 and -7 V, it is 0.1 and 0.2 eV less, respectively [18], than at U_b = 7 V, while as it was previously noted, it should not be lower. This result is due to the fact that the emission of secondary electrons from Ag NPs nanoparticles leads to the appearance of a negative charge in regions closed to them. The conclusion is supported by the fact that the relative intensities of the C-C/C-H state at U_b = 0 and -7 V are almost the same, i.e. their good conductivity is due to the presence of silver particles. In the case of U_b = 7, this effect was not observed because the intensity of the C-C/C-H state signal consists of signals from conducting and non-conducting areas. The presented results demonstrate the possibility of reliable analysis of chemical states of silver atoms from the O 1s spectra using the method of controlled differential charging.

Surface-sensitive XPS analysis shows that the treatment of the bandage with Ag-isopropanol organosol leads to presence of ~8.6 wt. % in the surface layer. However, bulk-sensitive X-ray fluorescence shows ~0.76 wt. %. This indicates that Ag NPs are stabilized mainly in the surface layer of the bandage (up to 8 nm).

Figure 2 shows the dynamics of changes in the area of aseptic wounds in relation to the initial one when different gauze medical bandages are applied over time.

Table 2 presents the data on the biochemical analysis of the blood of the experimental animals using conventional gauze medical bandage and containing Ag NPs.

Table 3 presents the parameters of white blood of experimental animals with the use of a conventional medical gauze dressing and containing Ag NPs.

When comparing the morphological picture of microscopic samples of wounds removed from the experiment on the 3rd day it was established that: (1) In the control group, detritus is defined in the

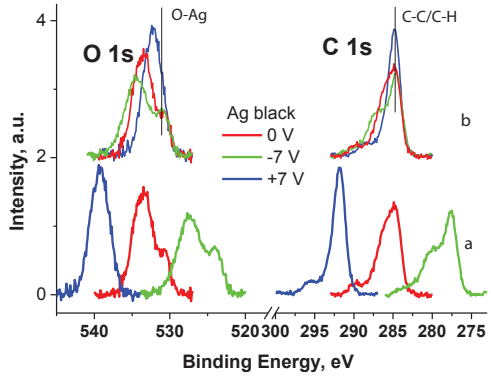

Figure 1: The O 1s and C 1s photoelectron spectra of Ag black measured at different Ub. The spectra (b) are the spectra (a) shifted by Ub value. The spectra are normalized by area under the spectral line to show there correspondence to same number of atoms.

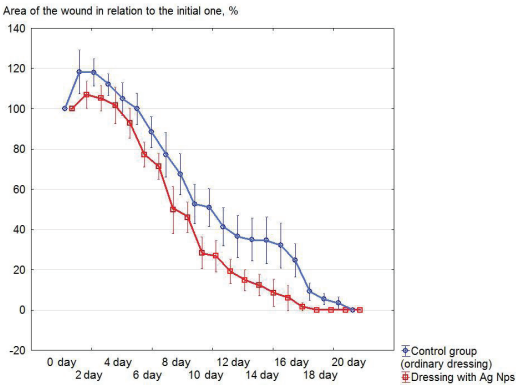

Figure 2: Dynamics of changes in the area of aseptic wounds with the use of various medical gauze dressings.

bottom of the wound in the form of a "broad band" densely infiltrated by neutrophils; pronounced edema. Diffuse leukocyte infiltration is observed in the wound edges up to the muscles. (2) The cellular composition in the polymorphic infiltrate consists of neutrophils, lymphocytes, macrophages and plasma cells. (3) With the approach to the center of the wound, the number of neutrophils increases. The newly formed capillaries are generally defined. They are expanded, sharply full-blooded, with marginal standing of leukocytes; the capillaries are located mainly along the periphery of the necrosis zone, which is an evidence of an exudative tissue reaction.

Compared with the changes in the control group, in the test group detritus was detected only in two cases in the form of a narrow strip. Fibrin was detected on the wound surface with a small number of neutrophils. In the underlying tissues there was a moderately pronounced edema and leukocyte infiltration (noticeably weaker than in the "control" group). These data indicate that the "cleansing" of the wound is carried out more vigorously.

Analysis of the histological picture on the 7th day showed that (1) in the control group, detritus with pronounced neutrophilic cell infiltration was recorded at the bottom and edges of the wound, but its thickness was 1.5 times less than on the third day; (2) in the underlying tissues up to the muscle, the growth of nonspecific granulation tissue was observed; it was consisted of a large number of newly formed capillaries and thick polymorphic cell infiltration.

Table 2: The main biochemical blood parameters of experimental animals with the use of various types of dressings.

Indicator	Group	Intact animals	The term of removal from the experiment			
			3 days	7 days	14 days	21 days
Bilirubin, μmol /L	control	2.70 (2.60; 2.85)	4.00$^{\$}$ (3.90; 4.20)	6.90$^{\$}$ (6.40; 7.10)	6.00$^{\$}$ (5.80; 6.10)	5.95$^{\$}$ (5.70; 6.10)
	experiment		6.00$^{\$*}$ (5.90; 6.30)	6.20$^{\$*}$ (6.10; 6.40)	7.05$^{\$*}$ (7.00; 7.10)	7.60$^{\$*}$ (7.40; 8.10)
ALT, U/L	control	66.50 (62.50; 75.00)	101.50$^{\$}$ (95.00; 103.00)	104.50$^{\$}$ (104.00; 110.00)	84.50$^{\$}$ (84.00; 86.00)	83.50$^{\$}$ (83.00; 85.00)
	experiment		110.50$^{\$*}$ (108.00; 113.00)	82.00$^{\$*}$ (81.00; 83.00)	71.00* (62.00; 77.00)	59.50* (51.00; 68.00)
AST, U/L	control	177.00 (172.00; 180.00)	214.00$^{\$}$ (210.00; 230.00)	268.50$^{\$}$ (260.00; 271.00)	192.50$^{\$}$ (182.00; 202.00)	191.00$^{\$}$ (181.00; 201.00)
	experiment		287.50$^{\$*}$ (266.00; 329.00)	175.50* (171.00; 181.00)	172.50* (168.00; 173.00)	173.00* (168.00; 175.00)
Protein, g/L	control	74.00 (70.50; 74.00)	56.50$^{\$}$ (56.00; 57.00)	64.50$^{\$}$ (63.00; 68.00)	66.00$^{\$}$ (65.00; 67.00)	70.00$^{\$}$ (70.00; 70.00)
	experiment		63.00$^{\$*}$ (63.00; 65.00)	70.00$^{\$*}$ (69.00; 71.00)	71.00* (71.00; 72.00)	72.50* (71.00; 73.00)
Glucose, mmol/L	control	9.05 (8.60; 9.80)	8.55 (8.40;8.70)	9.40 (9.30; 9.70)	9.65 (9.40; 10.60)	9.95 (9.40; 10.60)
	experiment		10.00$^{\$*}$ (9.80; 10.80)	10.20 (9.00; 10.50)	9.65 (9.30; 10.20)	9.90 (9.40; 11.30)
Urea, mmol /L	control	4.20 (3.50; 4.90)	4.85 (4.50; 5.10)	5.95$^{\$}$ (5.80; 6.30)	8.35$^{\$}$ (8.00; 8.50)	3.95 (3.60; 4.40)
	experiment		4.55 (4.40; 4.80)	5.00 (4.50; 5.40)	6.10$^{\$*}$ (5.50; 6.50)	4.40 (3.60; 4.70)
Creatinine, μmol /L	control	50.00 (47.50; 52.00)	45.50 (44.00; 55.00)	68.50$^{\$}$ (62.00; 70.00)	66.00$^{\$}$ (65.00; 68.00)	52.50 (52.00; 53.00)
	experiment		45.00$^{\$}$ (42.00; 47.00)	60.00$^{\$*}$ (57.00; 60.00)	66.00$^{\$}$ (63.00; 69.00)	54.00 (49.00; 55.00)

Notes: 1. $^{\$}$ - The data are statistically significant with respect to the intact animals ($p < 0.05$)
2. * - The data are statistically significant compared with the control ($p < 0.05$)

The morphological study showed that in comparison with the control group, in the test group, the epidermis is absent throughout the histologic sample. Compared with the control group, a large amount of detritus was observed in the bottom of the wound with pronounced neutrophilic cell infiltration. In the underlying dermis and adipose tissue (up to the muscle), nonspecific granulation tissue rich in cells and vessels was proliferating. The cells were dominated by lymphocytes and histiocytes. Fibroblasts and fibrocytes are determined moderately, isolated collagen fibers appear. Neutrophilic cell infiltrate extends to a depth of 1/3 of the dermis thickness.

Comparing the morphological picture of groups of animals derived from the experiment on 14th day, we note: (1) In the test group, in two cases, a wound defect is determined with the presence in the center of detritus with moderately pronounced leukocyte infiltration, growth of nonspecific granulation and young connective tissue. The wound is epidermized on ¾ of the area. The vascular component of granulation tissue is well expressed, especially at the border of the dermis and adipose tissue. Plasma cells are single. Compared to the "control" group, inflammatory infiltration is less pronounced, the collagen fibers are arranged more orderly. In the subcutaneous tissue, inflammatory changes were less pronounced (except for one case). (2) The growth of non-specific granulation and young connective tissue was observed in the dermis and subcutaneous tissue. The inflammatory infiltrate is rich in cells, among which lymphocytes, plasma cells, histiocytes, while fibroblasts and fibrocytes predominate. In five animals, collagen formation prevails over inflammatory infiltration, in one animal - *vice versa*.

On the 21st day, the morphological picture of the wounds of rats removed from the experiment, the control and test groups also differs (Figure 3 and 4).

In the preparations of the "control" group (Figure 3), the wound appears to be epithelialized, only in some places microscopic examination revealed the absence of the epidermis, on which and under which the leukocyte infiltration of different severity was contained.

In places where there was no epithelium, detritus with leukocyte infiltration was observed. In the underlying tissues in most cases thick lymphohistiocytic infiltrate was determined. The capillaries are reduced compared with those at the early stages of the wound and the proliferation of connective tissue is noted. In the test group (Figure 4), the wound appears to be epithelial throughout, however, in the underlying tissues, up to the muscle, an unevenly expressed lymphohistiocytic infiltrate (smaller compared to the control group) was determined. Vessels were determined in large numbers, dilated, full-blooded. The wound was filled with maturing connective tissue. Histopathological examination of the liver, kidney and myocardium revealed no pathological changes, which indicates the absence of a toxic effect of the dressing containing Ag NPs on these organs.

DISCUSSION

In accordance with the data, presented in figure 2, an increase in the wound area in relation to the initial one was observed in the first 4 days. The phenomenon was registered in all groups of animals. It was most and least significantly expressed in the control and test

Table 3: Indicators of leukocytes and leukogram of experimental animals when using different types of dressings.

Indicator	Group	Intact animals	The term of removal from the experiment			
			3 days	7 days	14 days	21 days
Leukocytes, ×10⁹/L	control	5. 70 (5.50; 5.90)	7.05 (5.40; 7.50)	10.30$ (10.20; 11.30)	12.55$ (11.30; 13.80)	7.60$ (750; 7.80)
	experiment		5.45 (5.30; 5.70)	6.90$* (6.80; 7.05)	11.00$* (10.60; 11.10)	5.95* (5.80; 6.10)
Stabs, %	control	1.00 (1.00; 1.00)	0.00 (0.00; 0.00)	0.00$ (0.00; 0.00)	0.00 (0.00; 1.00)	0.00 (0.00; 1.00)
	experiment		0.00 (0.00; 0.00)	0.00$ (0.00; 0.00)	0.00 (0.00; 0.00)	2.00* (2.00; 2.00)
Segmentated cells, %	control	29.50 (28.00; 30.00)	49.00$ (40.00; 54.00)	35.50 (33.00; 39.00)	29.00 (25.00; 30.00)	34.00$ (32.00; 35.00)
	experiment		36.50$* (36.00; 40.00)	32.00 (30.00; 37.00)	20.00$* (18.00; 20.00)	27.00* (26.00; 29.00)
Eosinophils, %	control	1.50 (1.00; 2.00)	2.00 (0.00; 3.00)	2.00 (0.00; 4.00)	0.50 (0.00; 2.00)	0.00$ (0.00; 0.00)
	experiment		2.00 (1.00; 2.00)	1.50 (0.00; 2.00)	2.00 (0.00; 2.00)	0.50 (0.00; 1.00)
Monocytes, %	control	2.00 (2.00; 2.00)	1.50 (0.00; 2.00)	2.00 (1.00; 3.00)	2.50 (2.00; 6.00)	4.00$ (3.00; 5.00)
	experiment		3.00$ (3.00; 3.00)	4.00$* (3.00; 4.00)	4.00$ (4.00; 4.00)	5.50$ (4.00; 7.00)
Lymphocytes, %	control	66.50 (65.00; 68.00)	48.00$ (41.00; 54.00)	60.00 (56.00; 62.00)	67.50 (66.00; 68.00)	61.00$ (59.00; 65.00)
	experiment		57.50$* (53.00; 58.00)	63.50 (58.00; 66.00)	75.00$* (74.00; 76.00)	65.00 (62.00; 66.00)
The leukocyte shift index by Yabuchinsky	control	0.49 (0.46; 0.52)	0.99$ (0.82; 1.33)	0.61 (0.56; 0.75)	0.41 (0.37; 0.47)	0.64$ (0.54; 0.68)
	experiment		0.65$* (0.61; 0.79)	0.51 (0.43; 0.64)	0.27$* (0.25; 0.27)	0.52 (0.48; 0.58)
Leucointoxic index	control	0.46 (0.41; 0.48)	0.97$ (0.72; 1.17)	0.55 (0.49; 0.64)	0.41 (0.35; 0.43)	0.52 (0.47; 0.55)
	experiment		0.57$* (0.56; 0.72)	0.47 (0.43; 0.59)	0.25$* (0.22; 0.25)	0.4* (0.38; 0.42)

Notes: 1 $ - The data are statistically significant with respect to the intact animals ($p < 0.05$)
2 * - The data are statistically significant compared with the control ($p < 0.05$)

groups by 18% and 7% increase, respectively. In the subsequent days of treatment up to complete healing, the reduction of the wound area relative to the initial one in the test group (bandage with Ag NPs) occurs more intensively, and the data are statistically significant with respect to the control. An experimental aseptic wound, tied with normal medical gauze dressing (control) and containing Ag NPs (test) was healed for 19.5 ± 0.34 and 16.17 ± 0.40, respectively.

The main biochemical parameters of the blood of experimental animals for various types of dressings are presented in table 2.

The level of bilirubin on the 3rd, 14th and 21st day in the test group is higher than in the control one, it decreases on the 7th day of the experiment. The dynamics of the activity of ALT and AST is similar: in all groups, its value decreases from the 7th to the 21st day. However, if on the 3rd day the activity of AST and ALT in the test group exceeds the control values, then from the 7th to the 21st day the activity of enzymes in the test group is below the control. It should be emphasized that on the 14th and 21st day in the test group, the activity of enzymes did not significantly differ from that of the intact animals, while in the control group, differences with the intact animals remained in all periods of the study.

The protein level in all groups from the 3rd to the 21st day of the experiment increases sequentially. From the 14th day in the test group, there were no significant differences in its content in comparison with the intact animals, while in the control group significant differences with these rats were recorded during all periods of the experiment. The level of protein in experimental animals exceeds the control values and approaches the level in the intact rats.

An increase in glucose level was registered only on the 3rd day in the group of animals treated with a dressing containing Ag NPs.

The level of urea on the 14th day in control animals is almost 2 times higher than in the intact rats. On the contrary, in the test group there was a significant decrease in this indicator, which reflects the normalization of the excretory function of the kidneys. It was established that creatinine level gradually increases from the 3rd to the 14th day of the experiment with the stabilization of this indicator by the 21st day. It should be noted that in all groups the level of creatinine on the 7th and 14th day is higher than that of the intact animals.

Table 3 presents the indicators of leukocytes and blood leukocyte formula of experimental animals when using different types of dressings. Analyzing the data, we can note that in all groups, the number of leukocytes from the 3rd to the 14th day increases, while decreasing was only by the 21st day. However, from the 7th to the 21st day, the number of leukocytes in the test group was significantly lower than that for the control.

The number of segmented neutrophils in all studied groups

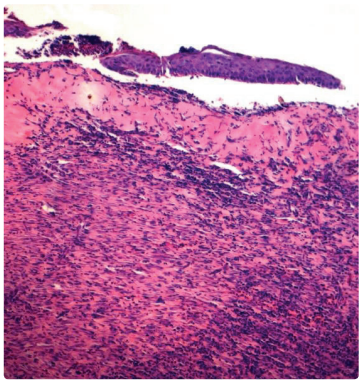

Figure 3: The bottom of the wound, in the treatment of which the ordinary dressing was used, the 21st day of the experiment. It was stained with hematoxylin and eosin, × 100.

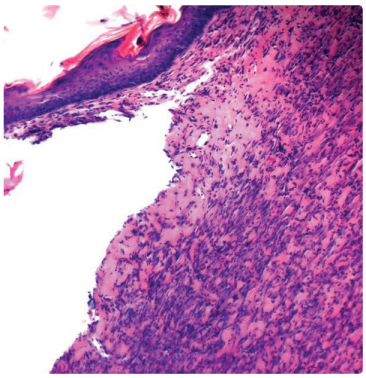

Figure 4: The bottom of the wound, in the treatment of which a dressing containing Ag NPs was used, the 21st day of the experiment. It was stained with hematoxylin and eosin, × 100.

decreased from the 3rd to the 14th day of the experiment. On the 21st day in the test group, their value does not differ from the values of the intact animals. The number of segmented neutrophils in all periods of the experiment in the test group, except for 7 days, was significantly lower than that of the control. Significant differences in the content of eosinophils in the studied groups were not identified.

In all groups of operated animals, a consistent increase in the level of monocytes from the 3rd to the 21st day of the experiment was observed. The number of monocytes exceeds the corresponding value in the intact animals in the test group at all times of the experiment, in control only on the 21st day.

The number of lymphocytes in the control and test groups increased from the 3rd to the 14th day. Moreover, their value in the test group on the 3rd and 14th was significantly higher than the control. By the 21st day there were no significant differences in lymphocyte content between the operated animals.

The leukocyte indices successively decreased from the 3rd to the 14th day in all animals with the experimental wound created. At the same time, in the test group on the 3rd and 14th day, their values were lower than the control ones. On the 21st day of the postoperative period, these indices did not significantly differ from those of the intact animals, except for the leukocyte shift index in the control group. Thus, it should be noted that an increase in the level of bilirubin in the test group on the 3rd, 14th and 21st day of the experiment indicates a positive effect of a dressing material containing Ag NPs on it. In turn, a decrease in the level of ALT and AST from the 7th to the 21st day of the study in the test group indicates the absence of toxic effects of nanoparticles on the liver cells.

Stabilization of the protein level in the test group in all periods of the study, compared with that of control, and the lack of significant differences in the protein content in both test groups, compared with the intact animals, indicates a positive effect of Ag NPs on the protein content. No Ag NPs effect on the glucose metabolism in the body is based on the absence of significant differences for the test, control, and a group of the intact animals during all periods of the experiment, excluding for the 3rd day. A significant decrease both in urea indices in the test group on the 14th day, and a decrease in creatinine content on the 7th day as well as the absence of statistically significant increases in these indicators in the test groups relative to those of the control indicate the absence of influence of a dressing material containing Ag NPs on the excretory function of the kidneys.

The use of medical gauze bandage containing Ag NPs is accompanied by a significant decrease in the number of leukocytes, the number of segmented neutrophils on the 7th - 21st day of the experiment. An increase in the number of lymphocytes and a decrease in the leukocyte shift index and leucointoxication index were observed on the 3rd and 14th days of the postoperative period, respectively. Throughout the experiment when using a dressing material with Ag NPs, no significant changes in the content of eosinophils were observed.

Our data suggest that when comparing the morphological picture of an aseptic wound, in the treatment of which the usual medical gauze dressing and a dressing containing Ag NPs were used, the latter type of one has a more pronounced positive effect on the healing of the aseptic wound during all periods of the study, manifested by acceleration regenerative process and faster wound healing.

CONCLUSION

Using an aseptic wound model in experiments on rats, a pronounced acceleration of healing with a dressing modified with Ag NPs compared to an ordinary dressing has been shown. The data is based on morphological, planimetric data and statistical analysis. Wound healing periods in the group with a normal medical gauze bandage and containing Ag NPs were 19.5 ± 0.34 and 16.17 ± 0.40 days, respectively.

The use of a dressing with Ag NPs leads to changes in the leukogram and leukocyte indices. The dressing material containing Ag NPs have no a toxic effect on the liver and kidneys cells, it does not affect the metabolism of glucose in the body of an experimental animal, and its use helps to normalize the level of total blood protein. The combination of the data confirms the validity of the use of nanomaterials based on medical gauze bandages containing Ag NPs for clinical testing. The effectiveness of the use of differential charging for discrimination Ag^0 and Ag^+ states has been shown.

ACKNOWLEDGEMENT

The contribution of Center for molecule composition studies of INEOS RAS is gratefully acknowledged. This investigation was carried out with the State Assignment of Fundamental Research to the A. N. Nesmeyanov Institute of Organoelement Compounds of the RAS. This research received no external funding.

REFERENCES

1. Akter M, Sikder MT, Rahman MM, Ullah AKMA, Hossain KFB, Banik S, et al. A systematic review on silver nanoparticles-induced cytotoxicity: physicochemical properties and perspectives. J Adv Res. 2018; 9: 1-16. https://goo.gl/M3ahc6
2. Allahverdiyev AM, Abamor ES, Bagirova M, Rafailovich M. Antimicrobial effects of TiO(2) and Ag(2)O nanoparticles against drug-resistant bacteria and leishmania parasites. Future Microbiol. 2011; 6: 933-940. https://goo.gl/P4gd9o
3. Niska K, Zielinska E, Radomski MW, Inkielewicz-Stepniak I. Metal nanoparticles in dermatology and cosmetology: interactions with human skin cells. Chem Biol Interact. 2018; 295: 38-51. https://goo.gl/PHY4wz
4. Vasil'kov AYu, Migulin DA, Naumkin AV, Belyakova OA, Zubavichus YV, Abramchuk SS, et al. Hybrid materials based on core-shell polyorganosilsesquioxanes modified with iron nanoparticles. Mendeleev Commun. 2016; 26**:** 187-190. https://goo.gl/UFB7MY
5. Abd-Elsalam KA, Vasil'kov AYu, Said-Galiev EE, RubinaMS, Khokhlov AR, Naumkin AV, et al. Bimetallic blends and chitosan nanocomposites: novel antifungal agents against cotton seedling damping-off. Eur J Plant Pathology. 2018; 151: 57-72. https://goo.gl/gMWZPx
6. Tsodikov MV, Ellert OG, Nikolaev SA, Arapova OV, Konstantinov GI, Bukhtenko OV, et al. The role of nanosized nickel particles in microwave-assisted dry reforming of lignin. Chem Eng J. 2017; 309: 628-637. https://goo.gl/XMA3Vv
7. Rubina MS, Kamitov EE, Zubavichus YV, Naumkin AV, Suzer SS, Vasil'kov AYu. Collagen-Chitosan Scaffold modifying with Au and Ag nanopatrticles: synthesis, structure and properties. Appl Surf Sci. 2016; 366: 365-371. https://goo.gl/pxQv92
8. Naidu KB, Govender P, Adam JK. Biomedical applications and toxicity of nanosilver: a review. Med Technol SA. 2015; 29: 13-19. https://goo.gl/fyhs2X
9. Koduru JR, Kailasa SK, Bhamore JR, Kim K, Dutta T, Vellingiri K. Phytochemical-assisted synthetic approaches for silver nanoparticles antimicrobial applications: a review. Adv Colloid Interface Sci. 2018; 256: 326-339. https://goo.gl/sxN6fi
10. Seil JT, Webster TJ. Antimicrobial applications of nanotechnology: methods and literature. Int J Nanomedicine. 2012; 7: 2767-2781. https://goo.gl/8zXuo2
11. Ivask A, Kurvet I, Kasemets K, Blinova I, Aruoja V, Suppi S, et al. Size-dependent toxicity of silver nanoparticles to bacteria, yeast, algae, crustaceans and mammalian cells in vitro. PloS One. 2014; 9: e102108. https://goo.gl/8vb9X2
12. You C, Han C, Wang X, Zheng Y, Li Q, Hu X, et al. The progress of silver nanoparticles in the antibacterial mechanism, clinical application and cytotoxicity. Mol Biol Rep. 2012; 39: 9193-9201. https://goo.gl/gXouAT
13. McShan D, Ray PC, Yu H. Molecular toxicity mechanism of nanosilver. J Food Drug Anal. 2014; 22: 116-127. https://goo.gl/Aqws3e
14. Ierano C, Peel T, Aytone D, Rajkhowa A, Marshall C, Thursky K. Surgical antibiotic prophylaxis-The evidence and understanding its impact on consensus guidelines. Infection, Disease & Health. 2018; 23: 179-188. https://goo.gl/tccFVP
15. Hall C, Allen J, Barlow G. Antibiotic prophylaxis. Surgery (Oxford). 2015; 33: 542-549. https://goo.gl/KGmX7
16. Simões D, Miguel SP, Ribeiro MP, Coutinho P, Mendonça AG, Correia IJ. Recent advances on antimicrobial wound dressing: A review. Eur J Pharm Biopharm. 2018; 127: 130-141. https://goo.gl/eDpfw
17. Naumkin A. Problems in Determination of Ag Charge State Atoms in Silver Nanoparticles by X-Ray Photoelectron Spectroscopy. Sci J Biomed Eng Biomed Sci. 2018; 2: 014-016. https://goo.gl/fi1iY
18. Vasil'kov AYu, Dovnar RI, Smotryn SM, Iaskevich NN, Naumkin AV. Plasmon resonance of silver nanoparticles as a method of increasing their antibacterial action. Antibiotics. 2018; 7: E80. https://goo.gl/7bkfz
19. Tjeng LH, Meinders MBJ, van Elp J, Ghijsen J, Sawatzky GA, Johnson RL. Electronic structure of Ag_2O. Phys Rev B Condens Matter. 1990; 41: 3190-3199. https://goo.gl/8jBcMx
20. Kaushik VK. XPS core level spectra and Auger parameters for some silver compounds. J Electron Spectrosc Relat Phenom. 1991; 56: 273-277. https://goo.gl/9kEiYx
21. Waterhouse GIN, Bowmaker GA, Metson JB. Oxidation of a polycrystalline silver foil by reaction with ozone Appl Surf Sci. 2001; 183: 191-204. https://goo.gl/d2ZYGk
22. Boronin AI, Koscheev SV, Zhidomirov GM. XPS and UPS study of oxygen states on silver. J Electron Spectrosc Relat Phenom. 1998; 2: 43-51. https://goo.gl/BRU1SV
23. Kaspar TC, Droubay T, Chambers SA, Bagus PS. Spectroscopic evidence for Ag (III) in highly oxidized silver films by X-ray photoelectron spectroscopy. J Phys Chem C. 2010; 114: 21562-21571. https://goo.gl/w1Bzi
24. Ferraria, AM, Carapeto AP, do Rego AMB. X-ray photoelectron spectroscopy: silver salts revisited. Vacuum. 2012; 86: 1988-1991. https://goo.gl/gAu3qV
25. Zhang F, Wu X, Chen Y, Lin H. Application of silver nanoparticles to cotton fabric as an antibacterial textile finish. Fibers and Polymers. 2009; 10: 496-501. https://goo.gl/6YyHso
26. Li G, Liu H, Zhao H, Gao Y, Wang J, Jiang H, et al. Chemical assembly of TiO_2 and TiO_2@ Ag nanoparticles on silk fiber to produce multifunctional fabrics. J Colloid Interface Sci. 2011; 358: 307-315. https://goo.gl/8TXbzZ
27. Xu H, Shi X, Ma H, Lv YH, Zhang P, Mao ZP. The preparation and antibacterial effects of dopa-cotton/AgNPs. Appl Surf Sci. 2011; 257: 6799-6803. https://goo.gl/8LFUS1
28. Kwak WG, Oh MH, Gong MS. Preparation of silver-coated cotton fabrics using silver carbamate *via* thermal reduction and their properties. Carbohydr Polym. 2015; 115: 317-324. https://goo.gl/VtRVy
29. Babu KF, Dhandapan, P, Maruthamuthu S, Kulandainathan MA. One pot synthesis of polypyrrole silver nanocomposite on cotton fabrics for multifunctional property. Carbohydr Polym. 2012; 90: 1557-1563. https://goo.gl/w14xpz
30. Xing Y, Yang X, Dai J. Antimicrobial finishing of cotton textile based on water glass by sol-gel method. J Sol-Gel Sci Technol. 2007; 43; 187-192. https://goo.gl/t8rD7
31. Su W, Wei S, Hu, SQ, Tang JX. Antimicrobial finishing of cotton textile with nanosized silver colloids synthesized using polyethylene glycol. J Textile Institute. 2011; 102: 150-156. https://goo.gl/QfpGRa
32. Kelly FM, Johnston JH. Colored and functional silver nanoparticle-wool fiber composites. ACS Appl Mater Interfaces. 2011; 3: 1083-1092. https://goo.gl/aAE7zu
33. He J, Kunitake T, Nakao A. Facile in situ synthesis of noble metal nanoparticles in porous cellulose fibers. Chem Mater. 2003; 15: 4401-4406. https://goo.gl/MKXfy
34. Bazant P, Kuritka I, Munster L, Kalina L. Microwave solvothermal decoration of the cellulose surface by nanostructured hybrid Ag/ZnO particles: a joint XPS, XRD and SEM study. Cellulose. 2015; 22: 1275-1293. https://goo.gl/pqbFx3
35. Ferraria AM, Boufi S, Battaglini N, Botelho do Rego AM, ReiVilar M. Hybrid systems of silver nanoparticles generated on cellulose surfaces. Langmuir. 2009; 26; 1996-2001. https://goo.gl/nHKd3
36. Beamson G, Briggs D. High Resolution XPS of Organic Polymers: The Scienta ESCA300 Database. Chichester: Wiley; 1992. p. 306. https://goo.gl/auzmB6
37. Samoilova N, Krayukhina M, Naumkin A, Yamskov I. Eco-friendly preparation of a magnetic catalyst for glucose oxidation combining the properties of nanometal particles and specific enzyme. Monatshefte für Chemie-Chemical Monthly. 2018; 149: 1179-1188. https://goo.gl/qALX3x
38. Da Silva O, Ohlsson A, Kenyon C. Accuracy of leukocyte indices and C-reactive protein for diagnosis of neonatal sepsis: a critical review. Pediatr Infect Dis J. 1995; 14: 362-366. https://goo.gl/uyLKChS